

Scintillation measurements during the EOPACE November '96 and August '97 campaigns

Arie de Jong, Marco Roos, Hans Winkel, Peter Fritz, Gerrit de Leeuw

TNO Physics and Electronics Laboratory
PO Box 96864, 2509 JG The Hague, The Netherlands
Tel: +31 70 374 04 56 Fax: +31 70 374 06 54 E-mail: deJong@fel.tno.nl

Paul Frederickson, Ken Davidson

Naval Postgraduate School
Code 63 DS, 589 Dyer Road Room 252, Monterey, CA 93493-5000

ABSTRACT

Following scintillation experiments during EOPACE measurement campaigns in the spring of 1996 [1, 2], a new set of experiments was designed in November 1996 and August/September 1997 over San Diego Bay. The main purpose was to further investigate the discrepancy between measured scintillation data and values predicted from turbulence models.

One simple way to measure scintillation was the decrease of the signal variations with increasing integration time in the IR transmissometer. In addition near-IR and midwave IR imagery was used of static and modulated sources. One of the static sources was mounted on a small boat, sailing out to horizon ranges, as was done earlier in the LAPTEX experiments at Crete [3]. For the detection of the signals of the modulated source a set of receivers was used, providing 2 lines of sight at different altitudes above the water.

The results show small differences in scintillation at 2 altitudes. The midwave and near-IR scintillation values show little correlation with C_N^2 values measured at the midway buoy, confirming the earlier experiments. The impact of atmospheric scintillation on IRST performance is again demonstrated.

Keywords: transmission, scintillation, boundary layer, infrared search and track, EOPACE.

1. INTRODUCTION

The importance of scintillation, due to atmospheric turbulence, for the performance of sensors detecting low altitude point targets at sea has been discussed before [2, 4, 5]. Due to the fact that modern sensors such as in Infrared Search and Track systems (IRST's) have high frame rates, the peak transmittance value is more important than the average transmittance. Experience learns that every few seconds the intensity of a near horizon target pops up by a factor of three or more above the mean intensity. Therefore knowledge of the frequency of occurrence of the transmission values is of greater importance than the Fourier spectrum. Figure 1a shows a typical transmission plot measured with a high speed transmissometer over the 15 km EOPACE path across San Diego Bay between the Naval Submarine Base and the Imperial Beach pier, reproduced from [2]. Figure 1b shows the corresponding histogram illustrating the above mentioned effect. A few remarks have to be made on this 'typical' result.

Firstly this transmissometer was operating at high speed and at a wavelength of 0.85 μm . The question rises whether the scintillation has the same magnitude at longer wavelengths, where future IRST's are assumed to operate (around 4 μm). According to the theory, scintillation decreases with increasing wavelength (see e.g. Beland [6]). However, this was not confirmed [2] by the measurements in Monterey, March 1996. Unfortunately, this comparison was not done with identical transmissometers.

The second remark concerns the Instantaneous Field Of View (IFOV) of the transmissometer. Most transmissometers have large IFOV's of several milliradians (mrad) while IR sensors tend to have IFOV's between 0.1 and 0.5 mrad. Point source contrasts in imaging sensors are generally measured by summing a certain number of pixel values in the immediate neighbourhood of the target and subtracting the background by summing the same number of background pixels having an average background value.

When this procedure is applied to focal plane array (FPA) cameras, care has to be taken, that scintillation effects are not influenced by the effect of the fill factor: the energy from the point target may partly fall between pixels, as described by Payne [7]. In our case however the IR FPA, used in the determination of scintillation has an optical blur greater than the pixel centre to centre distances, reducing the magnitude of this effect.

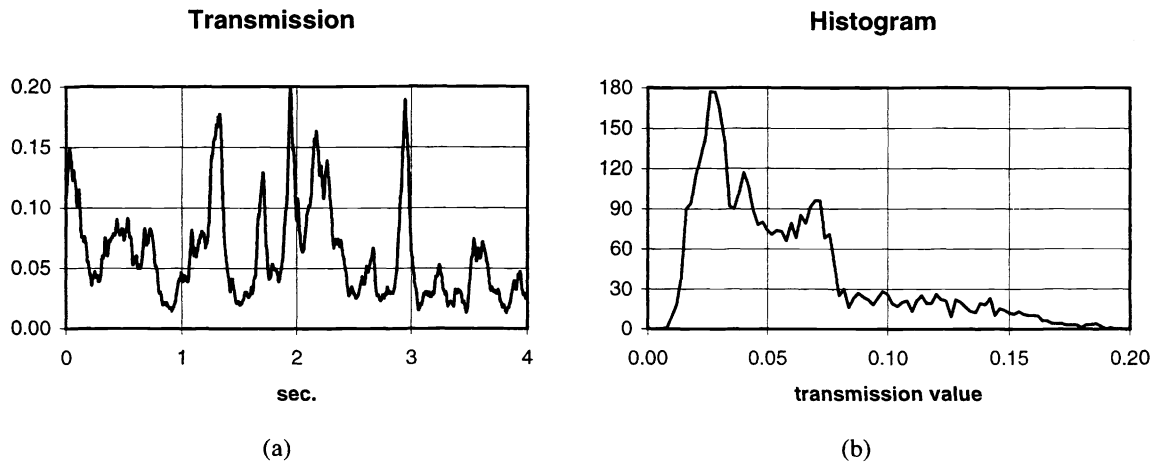


Figure 1.

a: Transmission plot 05-04-'96; local time 11:03:45; San Diego; 15 km; 0,85 μm .

b: Histogram of transmission data from figure 1a.

Associated with these remarks it was decided to introduce some new methodology and equipment in the third and fourth EOPACE transmission measurement campaigns in November 1996 and August/September 1997 in San Diego. The improved quality of the new scintillation data would also allow a more detailed validation of scintillation models, such as that from Kunz [8, 9], based upon bulk parameters.

A simple and straightforward method to quantify scintillation originates directly from the transmissometer set-up. As discussed elsewhere [1, 10] the midwave or longwave (MW, LW) IR signal is processed in a Lock-In amplifier with variable time constant. The normal time constant is 3 seconds, but the Signal to Noise ratio is sufficient for the use of a time constant of 0.1 second.

In addition a set of 4 receivers at 2 altitudes above the water was used, detecting the radiance of a modulated source. Scintillation was also measured by using a MW-IR camera and analysing the fluctuations in the peak signal, received from the fixed point source at the IB pier, and from a source mounted on a boat, sailing in and out from the Naval Sub-base.

The idea to measure scintillation at two heights stems from the strong variation of C_N^2 with height, as predicted by the bulk model. The comparison of scintillation measurements from imagery and scintillometers, allows (when data compare) the use of imagers and wide beam sources in open ocean conditions for carrying out similar experiments, which is difficult with standard scintillometers.

The use of MW-IR and near-IR instruments allows further investigation of the wavelength dependence of scintillation. Finally the set-up was designed to vary the centre distance between 2 TV camera's, both frame synchronised, for investigation of the correlation (if any) between scintillation along paths that are separated by small distances.

2. INSTRUMENTATION

The location of the transmission and scintillation measurements is illustrated in figure 2. The receivers were located in the BOQ of the Naval Submarine Base at Point Loma. In November the height of the receivers above mean sea level was 6.4 m and in August 6.4 and 9.4 m. The sources were mounted on the life guard station at the Imperial Beach pier at a height of 8.0 m above mean sea level. The distance between sources and receivers was 15.0 km. The minimum height of the lower line of sight (LOS) above mean sea level is 2.5 m. In the middle of the path, near the so called flux buoy from the Naval Postgraduate School, the water depth is about 21 m and the distance to the shore is about 4 km.

An instrumented boat, rented by SPAWAR, was making atmospheric characterization runs in both campaigns. In addition, in August/September 2 sources were mounted by TNO in a mast: a near-IR, 1000 Hz modulated source, at a height of 4.8 m above the water and a DC-IR source at a height of 4.3 m above the water. For the upper line of sight the horizon range to the DC-IR source is 17.8 km.

The sources at the IB pier consisted of a DC-visual/near-IR narrow beam (2°) alignment source, a 1623 Hz modulated visual/near-IR narrow beam (3.3×13 mrad) source for multipath scintillation measurements and an 820 Hz modulated IR source for standard IR transmission measurements with a beam width of 6.25 mrad. On the receiver site four near-IR telescopes (0.7-1.0 μm) were set-

up: two side by side (30 cm centre to centre distance) at the upper location and two at the lower location, especially for scintillation experiments. The IFOV of these telescopes was 9 mrad.

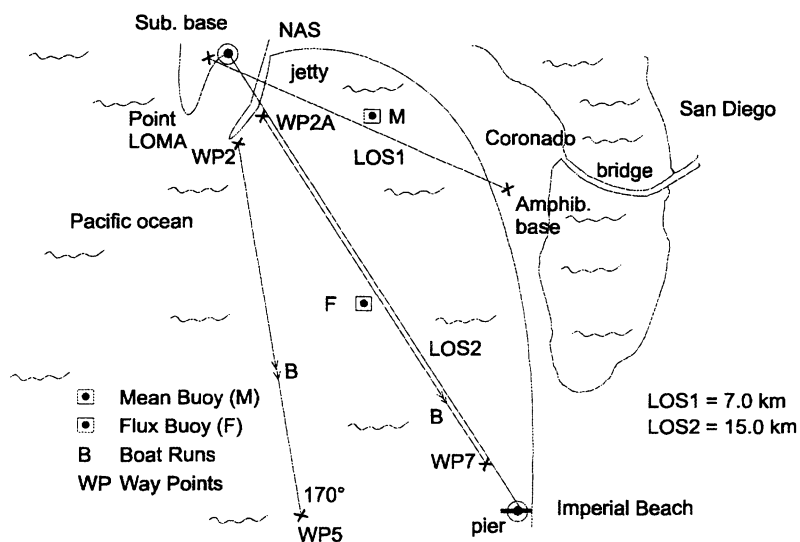


Figure 2. Location of the transmissometer line of sights over the San Diego Bay.

In addition, in August three telescopes were installed for standard transmissometry and also for MW-IR scintillation measurements: in the upper location a MW-IR detector (InSb), having an IFOV of 5 mrad, in the lower location an MW and LW-IR detector, having an IFOV of 4 mrad. The spectral bands for the MW and LW channels were resp 3.6-4.1 resp 8.0-13.1 μm . In November only the first telescope was mounted in the lower location. All telescopes used in the sources and receivers had a pupil diameter of 200 mm. For phenomenological survey and in part for scintillation experiments, two CCD camera's were installed at the lower location; provided with 300 mm lenses, their IFOV was about 30 μrad , sufficient to clearly identify refraction effects. In the upper location, in August, an MW-IR Thermacam PtSi (256 \times 256) FPA camera from Inframetrics was installed, with 8 $^\circ$ or 16 $^\circ$ FOV lens (IFOV resp 0.5 and 1.0 mrad), especially for scintillation measurements versus range.

For data acquisition a set of Lock-In amplifiers was used for the standard IR transmissometers. For the near-IR channels, sufficient signal to noise ratio was available from the 1623 Hz source to apply an auto-homodyne technique in software, near real time from the 12 bits recorded data. The Thermacam and CCD imagery was recorded on an SVHS videorecorder and acquired afterwards with a Matrox-METEOR frame grabber.

For more details of the set-up reference is made to [10]. For information on the results of the standard transmissometry reference is made to [11].

3. THE EXPERIMENTS

The scintillation measurements in November were primarily done with the standard transmissometer with .1 sec time constant and 9 Hz sampling rate. In total about 50 events have been selected, spread over the MW and LW bands, sometimes within a few minutes in order to compare the scintillation in both bands. In addition some scintillation measurements were carried out with the TV camera, sensitive in the near-IR (0.85 μm). A set of 150 images was read from the SVHS video tape for each event. The statistics of the apparent point source contrast for all frames was investigated for the selected events.

The scintillation measurements in August/September consisted of some continuous data collection experiments and some specially arranged events. The complete set of experiments is listed in table 1.

A number of boatruns was carried out from the jetty along the line of sight from the BOQ towards the IB pier, passing the flux buoy. A few runs were made along a line of sight from the BOQ into the direction 170 $^\circ$ until about 18 km. In total 25 runs were carried out from the early morning (05:00 local time) until the evening (18:00 local). For the days 29 and 31 August data were collected with both MW and near-IR.

Weather data, collected at the buoys by NPS (Paul Frederickson), were obtained from the EOPACE Web Site for both campaigns.

Table 1. List of scintillation experiments in August/September '97.

Sensor(s)	Description	Date	GMT
Near-IR scintillometer	24 hrs, each ½ hr; whole period; 1 channel	29/8-06/9	
2× Near-IR scintillometer	Correlation for 2 channels at 30 cm centre	29/8-06/9	
2× Near-IR scintillometer	1 upper and 1 lower line of sight	29/8-06/9	
MW-IR transmissometer	1 sec time constant; 20 events over 1 day	04/9	
MW-IR + Near-IR	4 channels parallel; 1623 Hz source	03/9	21:25
2× Near-IR scintillometer	Variation of pupil size: 20, 10, 5, 2.5 cm	02/9	01:17
1× Near-IR scintillometer	1000 Hz source on Explorer at ranges up to 15 km	29/8-04/9	
Thermacam	DC source on Explorer at ranges up to 15 km	26/8-31/8	
Thermacam + CCD camera	DC source on IB pier; MW/Near-IR comparison	02/9	16:22
CCD camera	Compare scintillation with Near-IR scintillometer	02/9	13:58
CCD camera	Source on Explorer at long range	28/8	18:45
CCD camera	Scintillation and mirage in fog	30/8	08:38

4. RESULTS

In November 1996 extremely refractive conditions occurred over San Diego Bay, as is illustrated by the pictures in figure 3. At the time of the pictures the air to sea temperature difference (ASTD) measured at the Flux buoy was about +4 K, providing superrefractive effects. The measured C_N^2 value (at the Flux buoy) was rising to values of $10^{-13} \text{ m}^{-2/3}$! The imagery, taken by the CCD camera of the point source at IB showed strong geometric blurring around 22:03 GMT of about 0.3 mrad. The average LW-IR transmission stayed however around the normal level of 20%, indicating no anomalies. However around 19:30 GMT the MW-IR transmission was boosted up above 100%, when the ASTD value was +1.7 K.

A representative set of MW and LW-IR scintillation data is listed in table 2. The table also contains data from the weather station of NPS at the Flux buoy. Quantifying scintillation as the ratio of the Standard deviation (Std) of the fluctuations in transmission and the Average (Avg) value of the of the transmission (in a period of 2 minutes), we find the Std/Avg ratio ranging between 0.10 and 0.29. Comparison with the C_N^2 values, taken at the same time, shows very little correlation. Also the ASTD values show little or no correlation with the scintillation.

Interesting is also the scintillation, found from the IR transmissometer by taking a longer time series. An example is presented in figure 4, where strong fluctuations in transmission within minutes occur due to large scale atmospheric instability. The ASTD was more than +5 K at this time and the wind was coming from the NW. The C_N^2 was about $10^{-13} \text{ m}^{-2/3}$. In the most extreme case the transmission increased more than a factor 10 within minutes.

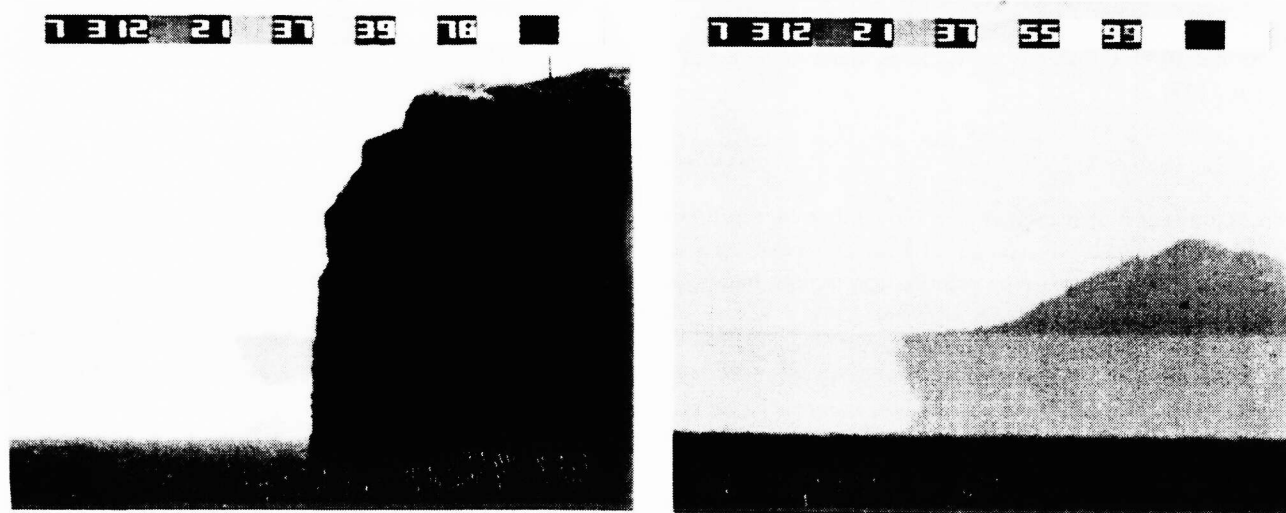


Figure 3. Coronado islands in refractive atmospheric conditions 07/11/96; 21:37 GMT; 2 horizons, separated 3.5 mrad, and strong mirages.

Table 2. List of MW and LW-IR scintillation data for November '96; 0.1 sec time constant.

Date	Time GMT	Spectral Band	Average transmission	Std/Avg	Max/Avg	ASTD	v_w	W_{dir}	C_N^2
05/11	22:55	MW	0.50	0.29	2.8	+1.1	3.3 m/s	267°	$0.31 \cdot 10^{-14} \text{ m}^{-2/3}$
05/11	23:15	LW	0.27	0.29	2.6				
08/11	07:03	MW	0.32	0.10	1.5	+2.2	3.3	57	$0.27 \cdot 10^{-13}$
11/11	19:00	LW	0.15	0.17	1.7	+3.7	2.6	278	$0.67 \cdot 10^{-13}$
13/11	18:10	MW	0.50	0.27	2.0	-0.2	1.7	266	$0.12 \cdot 10^{-15}$
13/11	14:30	MW	0.40	0.20	1.8	-1.0	2.1	263	$0.13 \cdot 10^{-14}$
15/11	14:55	LW	0.13	0.15	1.5	-0.7	4.6	226	$0.97 \cdot 10^{-15}$
15/11	15:05	MW	0.24	0.12	1.5				
17/11	06:40	LW	0.17	0.25	1.8	-1.4	2.7	78	$0.37 \cdot 10^{-14}$
18/11	14:55	LW	0.19	0.24	1.9	-1.7	2.0	68	$0.27 \cdot 10^{-14}$
18/11	15:05	MW	0.37	0.21	1.8				
20/11	00:05	MW	0.48	0.27	2.0	-0.6	4.9	335	$0.94 \cdot 10^{-15}$
20/11	14:55	MW	0.50	0.15	1.5	-1.2	4.6	14	$0.23 \cdot 10^{-14}$
20/11	15:05	LW	0.25	0.18	1.5				

The MW and LW scintillation data have been compared with some scintillation read-outs from the imagery of the CCD camera for the 8th and the 11th of November. Both data correspond reasonably well.

The results for the August/September campaign are presented in figures 5-16. Figure 5 shows an example of data from the 4-channel Near-IR scintillometer. The broadband transmission signal was sampled with a rate of 400 Hz. We can immediately conclude that the correlation of the data of 2 neighbouring channels (at 30 cm distance) is very low and that the scintillation in the upper and lower LOS is nearly the same. Figure 6 shows the histogram of the transmission data for the highest LOS, corresponding with the scintillation data in the upper plot of figure 5. Figure 7 shows the 24 hr Std/Avg data at each 1/2 hr for the whole campaign. The value of Std/Avg fluctuates between 0.1 and 0.45. Very little correlation was found with wind speed, ASTD or C_N^2 from the Flux buoy data cf. the C_N^2 plot for the same period in figure 8. The comparison of MW-IR and Near-IR scintillation with 4 telescopes with 20 cm diameter parallel at the lower LOS shows that the Std/Avg was within 10% for all channels (not shown).

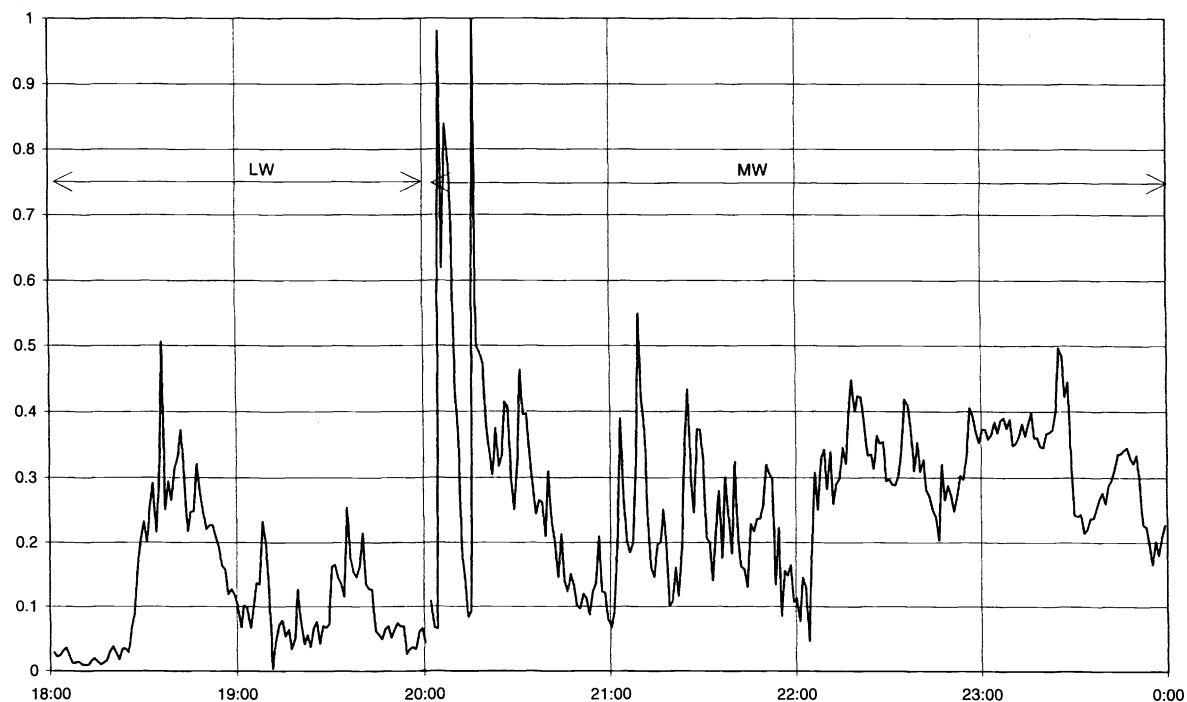
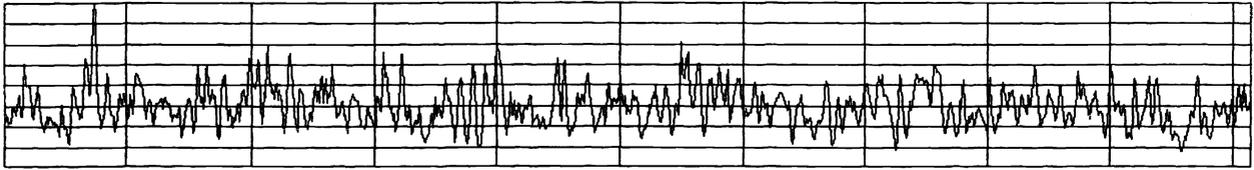


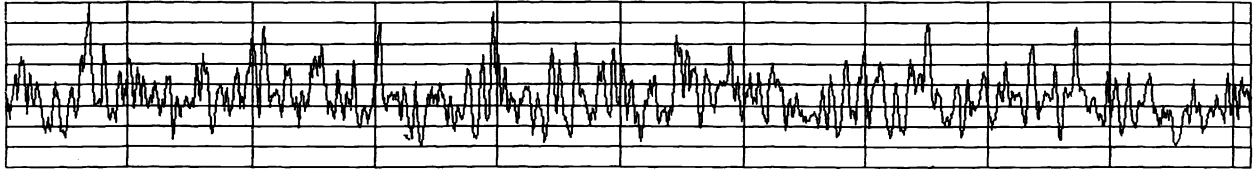
Figure 4. Example of longer time scale scintillation on 08/11/96.

TNO EOPACE * 28-08-1997 21:30:10 * 1623 Hz Imp. Beach

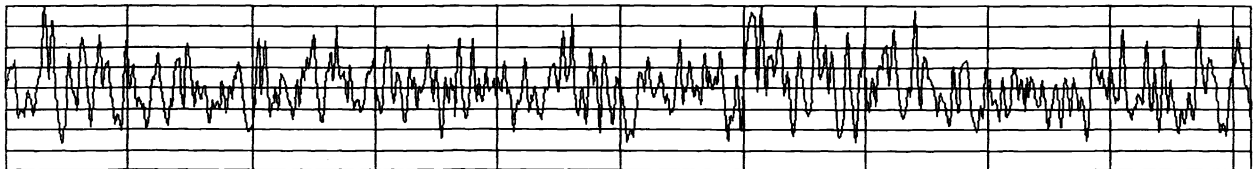
Top LOS NIR AVG=458,3 Max=1241 Min=70 STD=152,32 STD/AVG=0,33 pp/AVG=2,56 (max-avg)/AVG=1,71



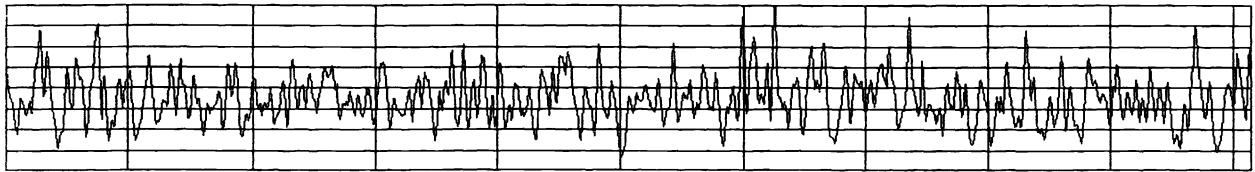
Top LOS NIR AVG=409,8 Max=971 Min=34 STD=136,59 STD/AVG=0,33 pp/AVG=2,29 (max-avg)/AVG=1,37



Low LOS NIR AVG=793,3 Max=1585 Min=94 STD=250,50 STD/AVG=0,32 pp/AVG=1,88 (max-avg)/AVG=1,00



Low LOS NIR AVG=1331,2 Max=3083 Min=130 STD=449,01 STD/AVG=0,34 pp/AVG=2,22 (max-avg)/AVG=1,32



1 sec / div.

Figure 5. Example of 4-channel Near-IR scintillometer-data; 28/08, 21.30 GMT (horizontal: time; vertical: transmission).

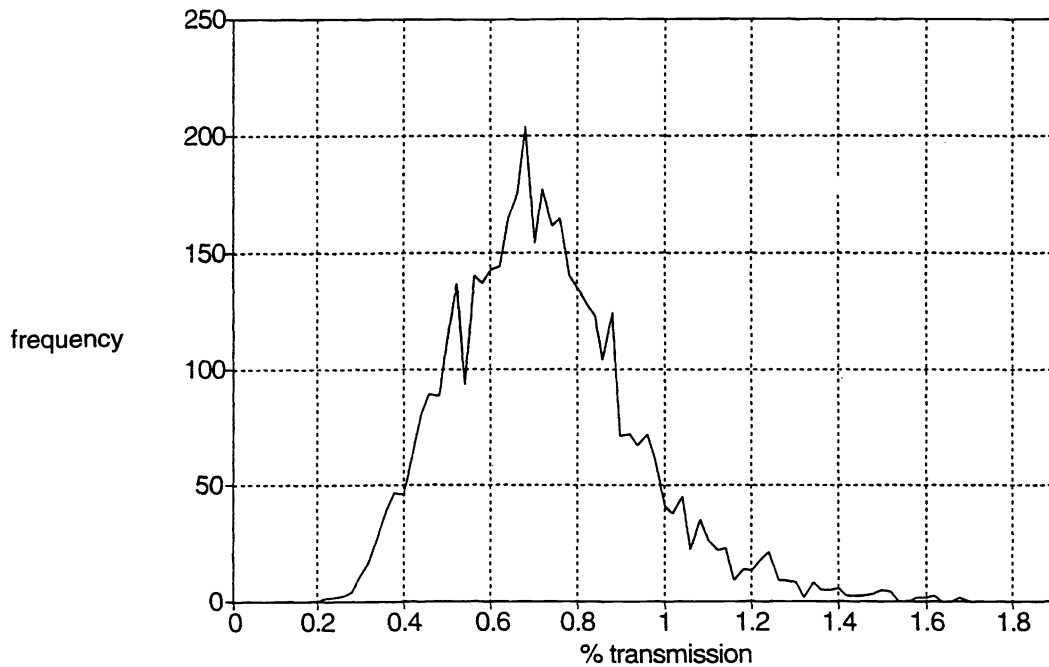


Figure 6. Histogram of near-IR transmission values; Top LOS (see figure 5) 28/08.

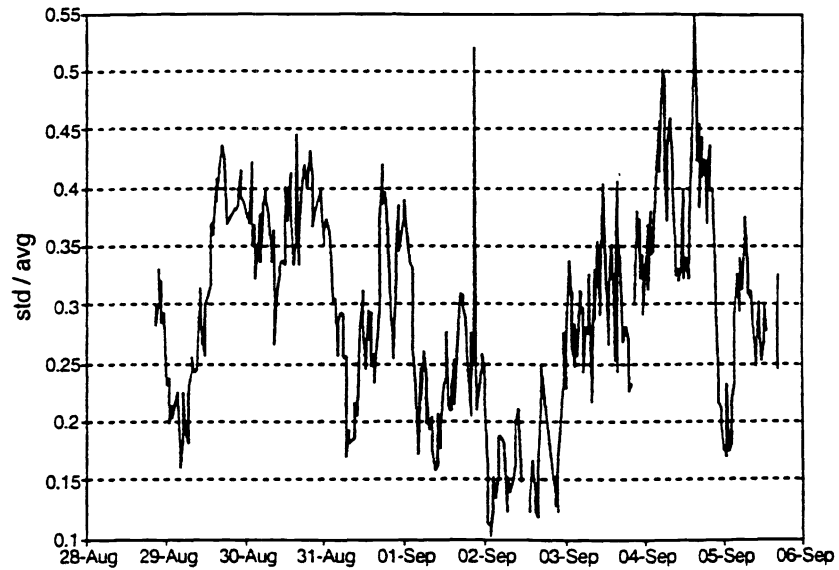


Figure 7. Scintillometer data (Top Line of Sight) for the whole period (August/September).

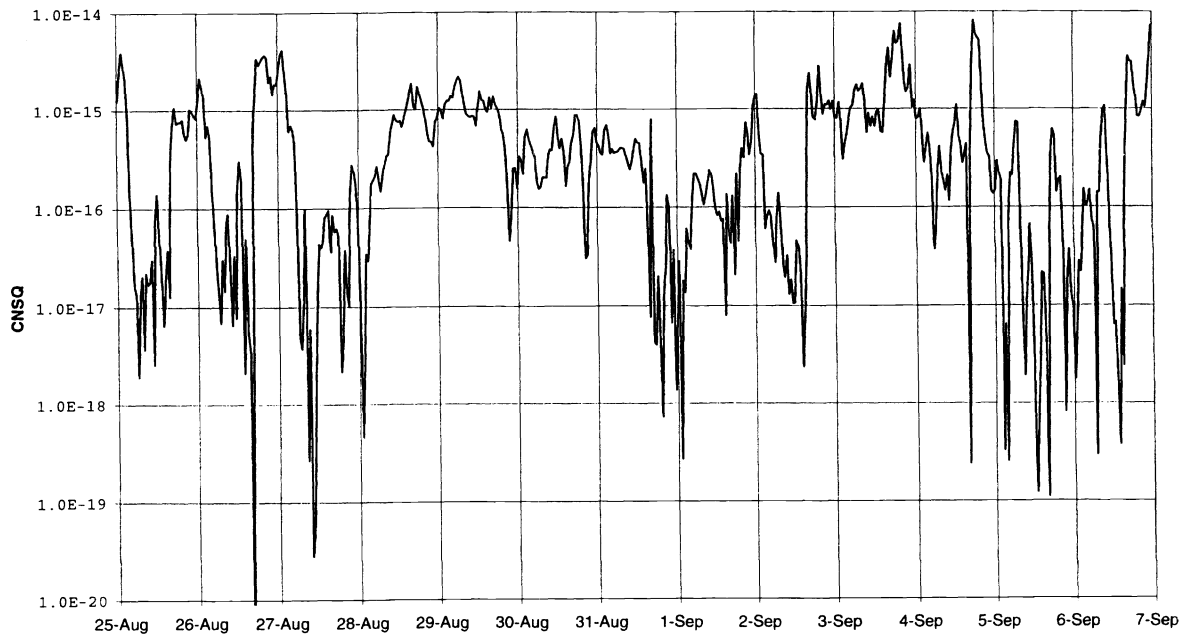


Figure 8. NPS-Flux buoy data: C_N^2 for whole period (August/September) in $m^{-2/3}$.

Figures 9, 10 and 11 show Near-IR and MW-IR scintillation data on the 31st of August and the 29th of August versus range by using the 1000 Hz source resp DC-IR source on the Explorer. We find an increase of scintillation with range, similar to the LAPTEX experiments [3]. The C_N^2 values from the Flux buoy during the experiments was $0.60 \cdot 10^{-15}$ resp $0.60 \cdot 10^{-17} m^{-2/3}$. The ASTD was close to zero for both cases. The Std/Avg ratio for both experiments had about the same value for the same range.

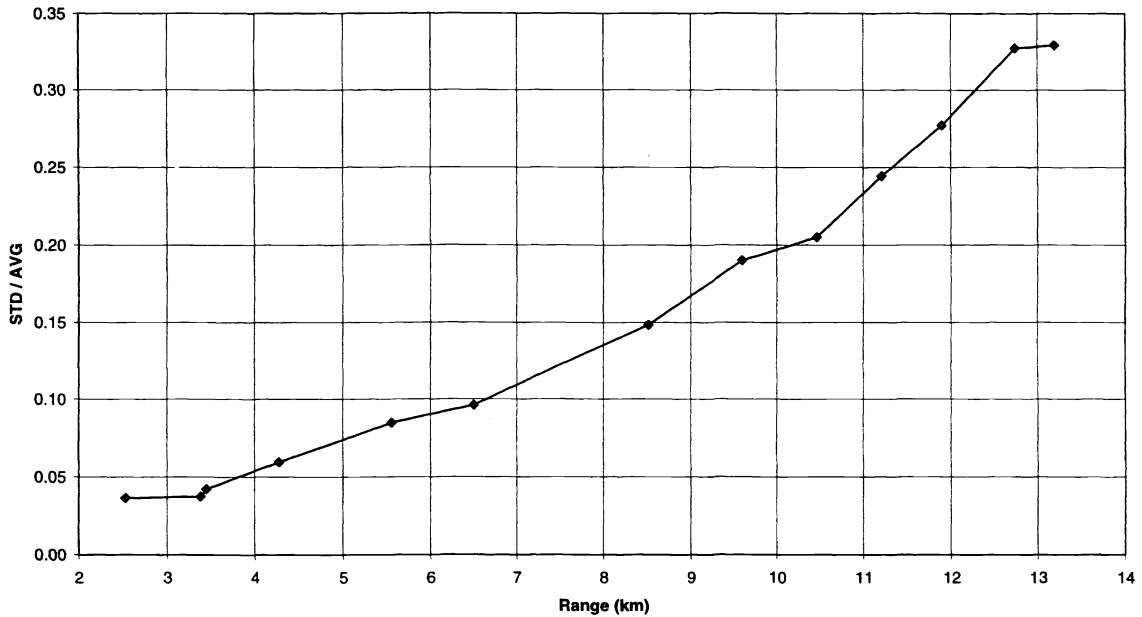


Figure 9. Near-IR scintillation versus range: 31/08, 23:00 GMT; Top LOS; 1000 Hz source.

Figure 10 with data from Thermacam imagery shows similar to figure 9 with data from the Near IR scintillometer an increase of scintillation with range. The average value is significantly higher than that measured with the modulated source. This difference is due to the scintillation of the background radiance of sources near the pier and the beach at Imperial Beach. Figure 11 does not show this effect due to the fact that the boat run was towards a sea background (WP5, see figure 2).

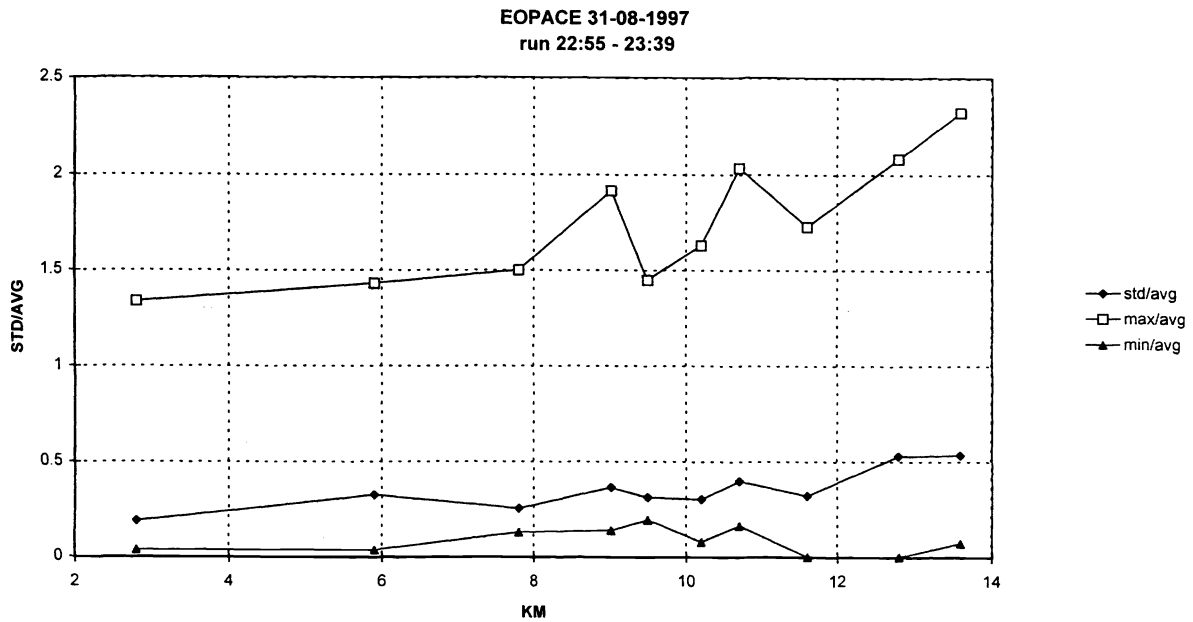


Figure 10. MW-IR scintillation versus range from Thermacam imagery during the same run as in figure 9: 31/08, 23:00 GMT.

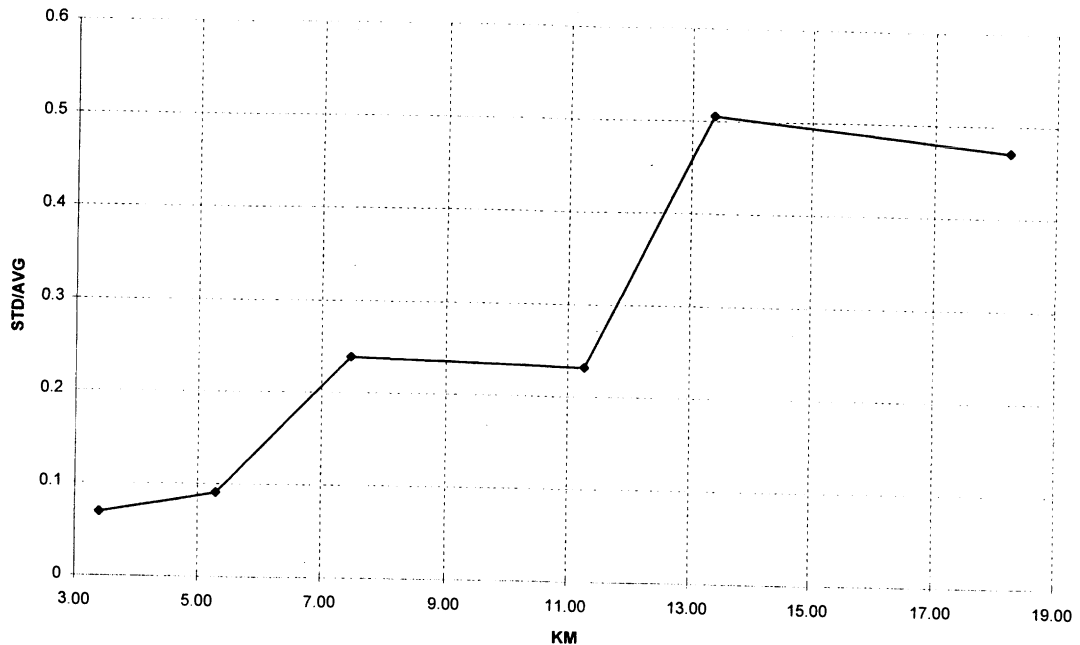


Figure 11. MW-IR scintillation versus range from Thermacam imagery; 29/08, 00:40 GMT.

More examples of the analysis of the Thermacam data are presented in figures 12 and 13. Figure 12 shows the Peak Difference of Sum (PkDOS) value for each of the 150 frames, which are taken with intervals of 0.2 sec (one out of 5 frames) during 30 seconds. The PkDOS is a bit value taken for a small rectangular area around the target, where the pixels are connected for the threshold, set above the background level and subtracting the background (sea, sky or land, depending on the scenario). The target is in the example of figure 12 at a range of 16.9 km, just before disappearing behind the horizon. At this range the scintillation tends to be the highest: $Std/AvG = 0.62$.

Figure 13 shows a histogram of all 150 PkDOS values for a typical data set at one range: 12.9 km. The histogram is again non-symmetric.

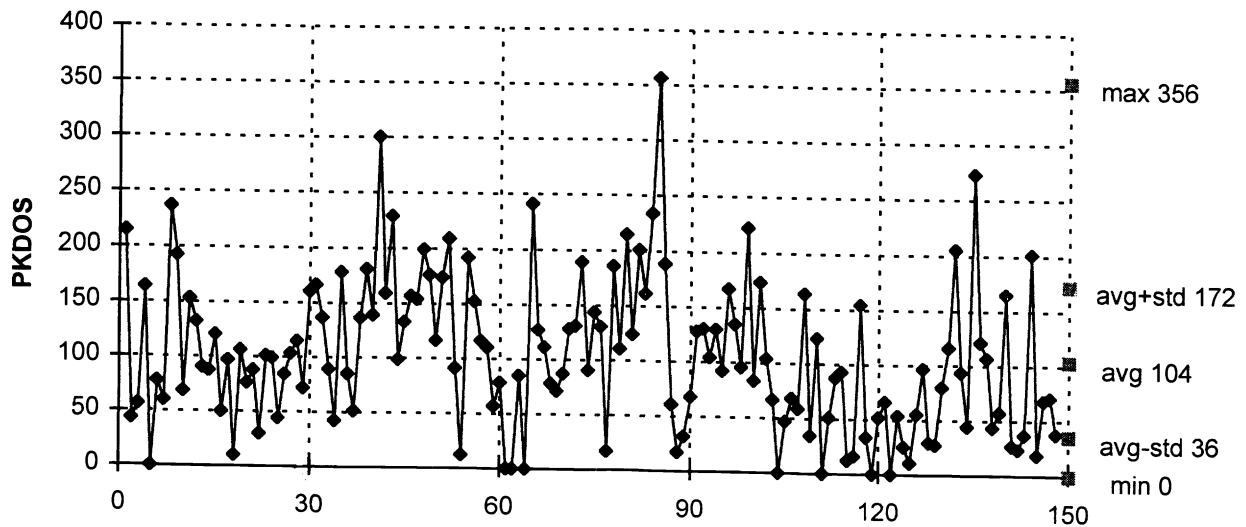


Figure 12. Peak Difference of Sum (PkDOS) values for 150 Thermacam images for Explorer at 19.6 km; 28/08, 12:30 GMT; $Std/AvG = 0.62$.

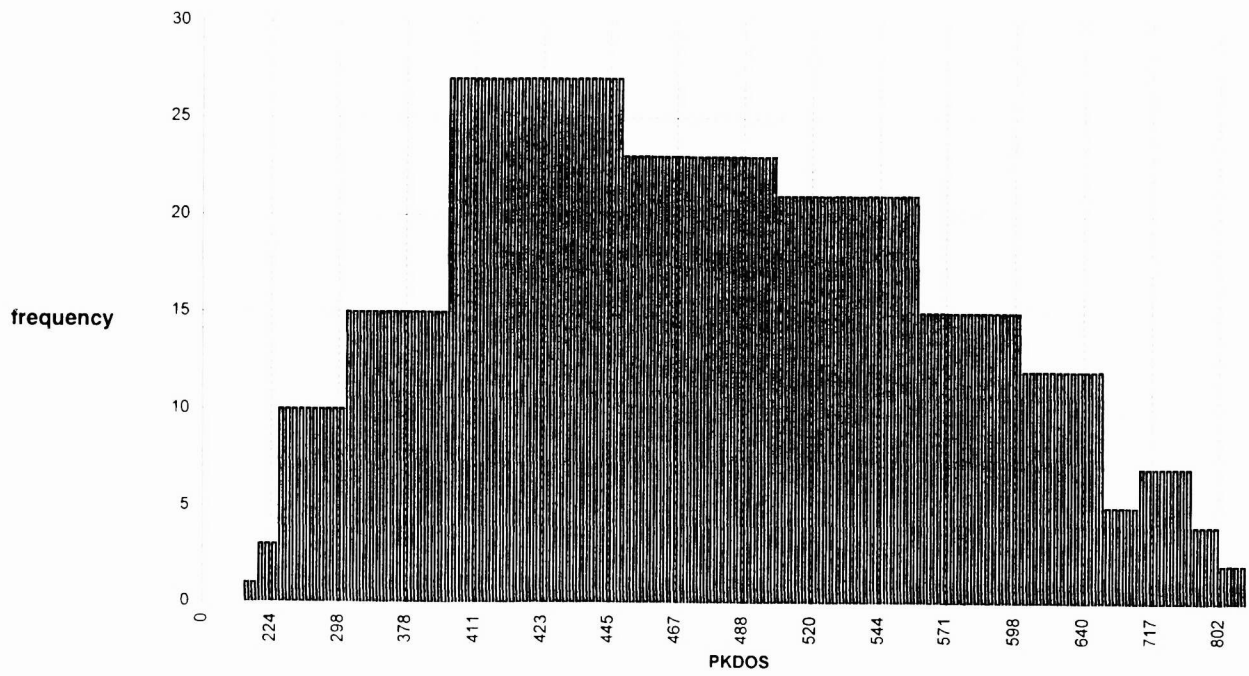


Figure 13. Histogram of PkDOS values for 150 Thermacam frames; Explorer at 12.9 km; 30/08, 00:35 GMT.

Table 3 contains scintillation data from the Thermacam camera at similar ranges for each of the boat runs for the period 26/08-31/08. It is found that scintillation values S^{std}/Avg are strongly variable, not corresponding with the C_N^2 data from the Flux buoy. Figure 14 shows some MW-IR pictures, taken with 0.2 sec intervals. The target is the point source at the IB pier (15 km). The atmospheric condition is somewhat sub-refractive at this time (ASTD = -0.6 K) resulting in mirage effects, just discernible in the Thermacam with 0.5 mrad IFOV. The effect results in strong intensity variations, shown in the figures.

Table 3. Thermacam scintillation data for 14 boat runs at ranges between 11.5 and 16.3 km; comparison with C_N^2 data (in $m^{-2/3}$) from Flux buoy.

Data boat runs with Thermacam											
data	start local time	sample UTC time	distance	AVG	STD	MAX	MIN	STD/AVG	CN ²	background	
26/08	4:47	12:29:11	14.4 km	376	84	541	118	0.223	4.80E-17	sky	
26/08	15:10	23:00:53	16.3 km	24	26	200	0	1.12	8.70E-16	sky	
27/08	6:10	13:48:49	14.5 km	147	35	239	83	0.236	2.10E-18	sky	
27/08	8:50	16:20:57	13.2 km	276.6	37.1	352.6	155.4	0.134	6.60E-16	sky	
27/08	13:34	21:10:10	14.5 km	44.2	54	268	0	1.221	1.90E-15	sky	
27/08	17:45	1:22:06	13.4 km	180.4	95.6	388.3	20.9	0.5297	4.20E-15	sky	
28/08	5:00	12:15:11	16.2 km	266.5	54.2	411.5	128.3	0.203	4.00E-17	sky	
28/08	8:41	15:57:28	13.0 km	361.8	153.2	770	35	0.42	8.50E-17	sky	
28/08	15:00	22:36:12	13.5 km	183.8	37.9	317.5	58.9	0.206	2.30E-16	sky	
28/08	18:10	1:43:38	13.0 km	62.6	65.9	327.3	0	1.053	3.50E-18	sky	
29/08	6:30	13:56:25	12.0 km	413.2	122	765.6	97.7	0.2971	6.60E-16	sky	
29/08	9:30	16:57:26	12.2 km	245.5	132.2	571.2	0	0.538	1.10E-15	land	
				175.5	112.4	457.7	0	0.64		sky	
29/08	17:00	0:35:08	12.9 km	443.9	141.2	834.9	118.7	0.318	1.00E-15	land	
				499.8	144.7	896	149	0.289		sky	
31/08	15:55	23:28:12	11.5 km	308.2	128.9	713	73.5	0.418	6.30E-16	land	
				449.8	144.6	867.5	138.8	0.321		sky	
				615.1	166.1	1047.6	198.8	0.27		sea	

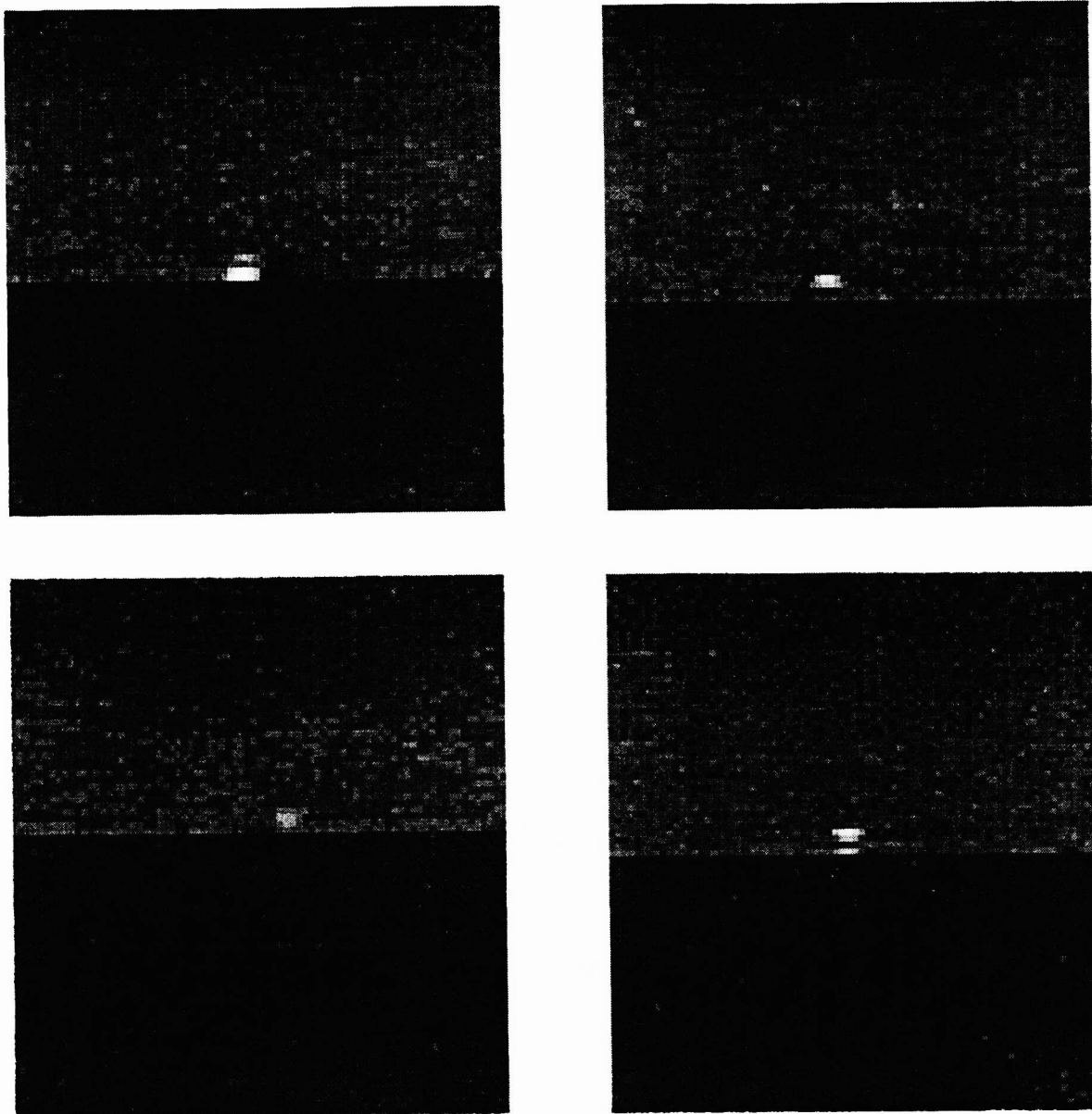


Figure 14. Four Thermacam frames at 0.2 sec interval with point source at IB pier; 15 km; 31/08; 23:24 GMT.

Figure 15 shows the scintillation data from the MW-IR transmissometer for the 4th of September, similar to table 2. The figure shows a decrease in transmission in the course of the day and a decrease of the scintillation, probably due to a reduction of the visibility. Again little correlation with C_N^2 data is observed, although a slight trend exists.

The experiment with variation of pupil size was done 2 times. The results are listed in table 4. The results show an expected increase in scintillation. For the smallest pupil the scintillation is entering the saturation zone. The data were taken for the upper LOS. Table 5 shows sample results of scintillation measurements with the CCD camera with near-IR filter, and the MW-IR Thermacam camera. Care was taken that the signal of the point source did not saturate in the video channel. For this purpose the pupil of the CCD camera was reduced to 5 mm diameter, when recording the source at the pier.

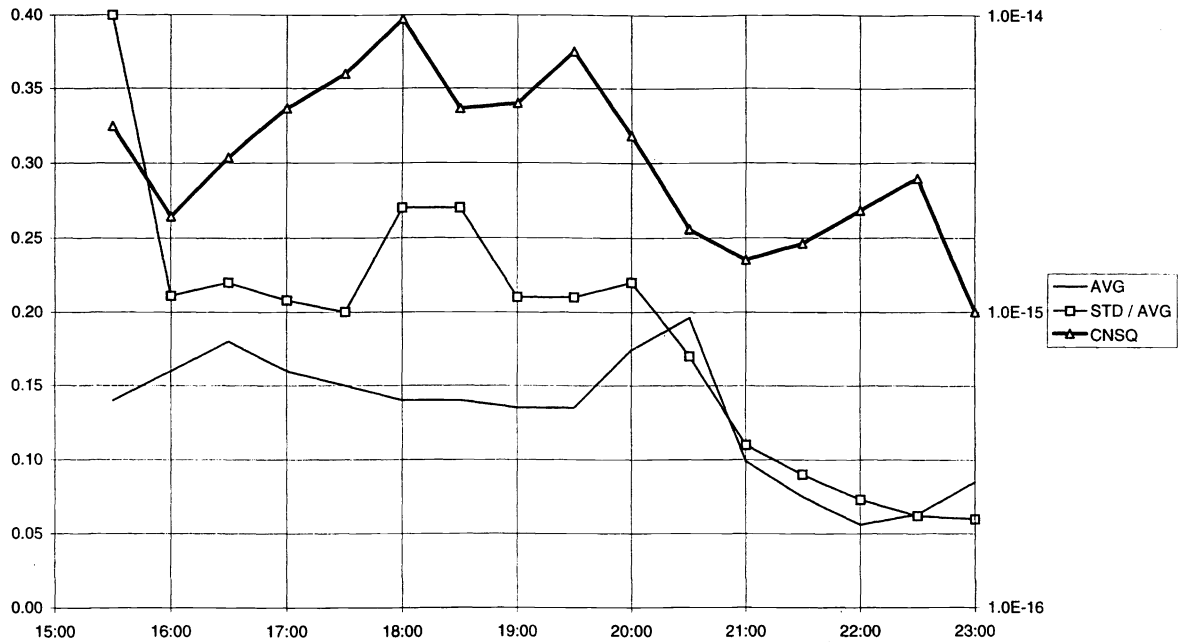


Figure 15. Average transmission and Std/Avg value for MW-IR, Top LOS with 0.1 sec integration time from standard transmissometer; 04/09, 15:30-23:00 GMT.

Table 4. Results of experiments with variable pupil size on scintillometers.

Date	Time (GMT)	Pupil diameter	Std/Avg	ASTD	C_N^2
01/09	20:08	20 cm	0.25	+0.2 K	$0.15 \cdot 10^{-16} m^{-2/3}$
	20:09	10	0.40		
	20:12	5	0.62		
02/09	01:17	20	0.16	+0.1 K	$0.18 \cdot 10^{-16}$
	01:20	10	0.25		
	01:21	5	0.37		
	01:23	2.5	0.60		

Table 5. Set of scintillation recordings with CCD near-IR and Thermacam (MW-IR).

Date	Time (GMT)	Camera	PkDOS Std/Avg	Source	Range (km)	ASTD (K)	C_N^2	v_w	W_{dir}
28/08	18:40	Near-IR		Boat	14	+0.1	$0.2 \cdot 10^{-17} m^{-2/3}$	1.1 m/s	311°
29/08	14:54	MW-IR	0.16	Pier	15	-1.5	$0.12 \cdot 10^{-14}$	2.5	343
29/08	16:48	MW-IR	0.45	Pier	15	-1.7	$0.11 \cdot 10^{-14}$	1.8	333
31/08	00:18	MW-IR	0.26	Pier	15	-0.4	$0.33 \cdot 10^{-15}$	4.9	6
31/08	23:24	MW-IR	0.29	Pier	15	-0.7	$0.63 \cdot 10^{-15}$	4.8	3
02/09	13:58	Near-IR		Pier	15	-0.3	$0.75 \cdot 10^{-16}$	3.0	276
02/09	15:18	Near-IR		Boat	14	+0.3	$0.13 \cdot 10^{-15}$	3.3	281
02/09	15:46	Near-IR		Pier	15	+0.2	$0.54 \cdot 10^{-16}$	2.3	249
02/09	16:14	MW-IR		Pier	15	+0.2	$0.13 \cdot 10^{-15}$	1.7	263
02/09	16:15	Near-IR		Pier	15	+0.2	$0.13 \cdot 10^{-15}$	1.7	263
02/09	16:26	Near-IR		Pier	15	+0.2	$0.13 \cdot 10^{-15}$	1.7	263

5. DISCUSSION AND CONCLUSIONS

Following the generally accepted theory [6, 9] the standard deviation σ_χ of the propagation constant depends on wavelength λ , range R , distance integration variable r and refractive index structure function parameter as follows:

$$\sigma_\chi^2(R) = 0.56 \left(\frac{2\pi}{\lambda} \right)^{7/6} \int_0^R C_N^2(r) \left(\frac{r}{R} \right)^{5/6} (R-r)^{5/6} dr \quad (1)$$

$\sigma_\chi(R)$ is approximately proportional to the standard deviation of the intensity fluctuations Std and the average intensity Avg , used in the results. In formula (1) the middle part of the measurement path is weighed more than both ends. In view of this, the location of the flux buoy midway is correct for measuring the value of C_N^2 .

If we consider C_N^2 to be a constant over the range R gives a simplification of formula (1):

$$\left(\frac{Std}{Avg} \right)^2 = 0.496 C_N^2 \left(\frac{2\pi}{\lambda} \right)^{7/6} R^{11/6} \quad (2)$$

If we take from figure 7 the average value of $Std/Avg = 0.3$, for $\lambda = 0.85 \cdot 10^{-6}$ m, for $R = 1.5 \cdot 10^4$ m we find the value C_N^2 should have: $0.4 \cdot 10^{-16} \text{ m}^{-2/3}$. The measured value of C_N^2 is fluctuating between 10^{-15} and 10^{-16} , which is too high, but better than the value measured in April 1996. Also the fluctuations in C_N^2 do not correspond with the fluctuations in (Std/Avg) over the whole period, although for the 2nd of September the Std/Avg value is about 0.15, corresponding to a C_N^2 value of $10^{-17} \text{ m}^{-2/3}$, which corresponds somewhat better than for the rest of the period.

Also a comparison between (Std/Avg) values measured and the ASTD values learns that the predictions are at least incorrect for ASTD values close to zero, resulting in near zero C_N^2 values and thus low scintillation, also found in [12].

Similar to the results of previous EOPACE campaigns [2], the results from table 2 and the data from the MW and near-IR measurements on the 1623 Hz source on the pier show no dependence of scintillation on wavelength, at least not for the 20 cm pupil size and the atmospheric conditions over the San Diego Bay. This means that formula's (1) and (2) do probably not apply for these conditions, because the ratio of LW and MW-IR wavelength is about a factor 3 and between MW and near-IR a factor 4.5. The scintillation according to formula (2) should have a ratio of $\sqrt{3.6}$ resp $\sqrt{5.8}$, which is not found; we found ratio's of nearly 1.

Striking is the longer term 'scintillation' type of effect, frequently found in the refractive conditions in November. Longer term means here minute scale instead of second scale.

The 4 channel scintillometer further learned that the scintillation values were within 10% for the upper and lower LOS. This is in contradiction with model prediction [9] describing the dependence of C_N^2 with height. In the central part of the LOS the height of the LOS above the water is 2.5 resp 4 m for the lower resp upper LOS. For this condition the lower LOS would face a C_N^2 value of about 2 times higher than the upper LOS and thus the scintillation would be $\sqrt{2}$ times higher.

Another important issue, coming out of the 4 channel scintillometer was the lack of correlation of the transmission of 2 neighbouring devices at 30 cm centre distance, which is important in systems, where processing of the signals of 2 parallel sensing devices is carried out.

Scintillation is increasing with smaller pupil sizes, as can be expected from the pupil averaging affect. This by the way can nicely be visualised at night, by observing the intensity fluctuations on a screen out of focus of the receiver optics.

Scintillation is also increasing with range in a nearly linear way, which corresponds with the prediction in formula (2). This increase is as well found from the near-IR scintillometer and the modulated source on the boat, as well as from the MW-IR imager, using digital image analysis software. Although the latter method is more time consuming and may include small uncertainties due to background effects (such as in the case of land background), longer ranges can be achieved because of a better signal to noise ratio. Another advantage is the wider beam divergence of the DC source than the modulated source; therefore boat motions have less effects on the signal strength. Therefore, as seen earlier in LAPTEX [3], imagery allows scintillation measurements to the horizon. This is of special interest, because it was found that strong scintillations frequently occur just before appearing or disappearing of the source, indicating that the lowest layer (1-20 cm) above the water can provide the strongest temperature gradients.

The statistics of the scintillation, as measured with a MW-IR Focal Plane Array camera, show that for medium ranges of about 15 km the ratio of the maximum PkDOS value and the average PkDOS value is about 2 to 3, with in some cases a value of 5 and more close to the horizon. This has an impact on the threshold of future IRST's for long range target detection at sea.

It is not sure that the scintillation effects, measured in the coastal environment, will be the same in open ocean conditions. It would be interesting to make experiments at open sea with a wide beam IR source on one ship and an MW-IR camera on a second ship at variable ranges. Clear separation of the DC source from the rest of the ship is rather essential for reliable signal analysis.

6. ACKNOWLEDGEMENTS

The EOPACE activities of TNO-FEL are supported by the Netherlands Ministry of Defence, project A95KM729 and the US Office of Naval Research, grant N00014-96-1-0581.

Great support for the experiments was received by personnel from SPAWAR, San Diego, in particular Doug Jensen for his support in the arrangements and Stu Gathman, Charly McGrath and Kathleen Liffittin for their support in the measurements.

Personnel from the Bachelor Officers Quarter (BOQ) at the Naval Submarine Base and the Life Guard Station at Imperial Beach are acknowledged for their great support.

At TNO-FEL Ruud Kooyman and Maarten Zwaan are greatly acknowledged for their support in preparing the measurement equipment. Marcel Moerman is acknowledged for his support in gathering weather data during the experiments and participation in a large part of the experiments.

7. REFERENCES

[1] A.N. de Jong et al, *EOPACE Transmission Experiments Spring '96, Preliminary Results*, TNO report FEL-96-A090, October 1996.

[2] A.N. de Jong et al, *Low elevation transmission measurements at EOPACE, Part III: Scintillation effects*, SPIE proceedings Vol 3125, San Diego, July 1997.

[3] A.N. de Jong et al, *Point target extinction and scintillation as function of range at LAPTEX, Crete*, SPIE proceedings Vol 3125, San Diego, July 1997.

[4] T.L. Klein et al, *Characteristics of 3-5 μm scintillation at low altitudes in a coastal marine environment*, Proceedings IRIS meeting, Albuquerque, January 1996.

[5] D.L. Marable et al, *Incorporation of scintillation in IR detection and track models for low altitude targets in a marine environment*, Proceedings IRIS meeting, Albuquerque, January 1996.

[6] R.R. Beland, *Propagation through Atmospheric Optical Turbulence*, The IR and EO systems Handbook: Vol 2, pp 157-232, SPIE Optical Engineering Press, 1993.

[7] T.M. Payne, *Apparent scintillation of subpixel targets imaged by focal plane arrays*, Optical Engineering Press, 36(1), January 1997.

[8] G.J. Kunz, *Validation of a bulk turbulence model with thermal images of a point source*, SPIE proceedings Vol 2828, Denver, August 1996.

[9] G.J. Kunz, *A bulk model to predict optical turbulence in a marine surface layer*, TNO report FEL-96-A053, April 1996.

[10] A.N. de Jong et al, *Transmission experiments during EOPACE, November 1996 and August/September 1997, Preliminary Results*, TNO report FEL-97-A269, January 1998.

[11] A.N. de Jong et al, *Long-range transmission at low elevations over the ocean*, Proceedings NATO-SET Symposium on 'EO Propagation, Signature and System Performance', Naples, March 1998.

[12] P. Frederickson, K.L. Davidson, *Near-Surface Scintillation (C_n^2) Estimated from a Buoy During EOPACE*, Proceedings NATO-SET Symposium on 'EO Propagation, Signature and System Performance', Naples, March 1998.